Heterojunction of FeOOH and TiO$_2$ for the Formation of Visible Light Photocatalyst

Sher Bahadur Rawal, Ashok Kumar Chakraborty, and Wan In Lee*

*Department of Chemistry, Inha University, Incheon 402-751, Korea. *E-mail: wanin@inha.ac.kr*
Received July 6, 2009, Accepted September 9, 2009

FeOOH/TiO$_2$, a heterojunction structure between FeOOH and TiO$_2$, was prepared by covering the surface of the ~100-nm-sized FeOOH particles with Degussa P25 by applying maleic acid as an organic linker. Under visible light irradiation ($\lambda \geq 420$ nm), FeOOH/TiO$_2$ showed a notable photocatalytic activity in removal of gaseous 2-propanol and evolution of CO$_2$. It was found that FeOOH reveals a profound absorption in the spectral range of 400 - 550 nm, and its valence band (VB) level is located relatively lower than that of TiO$_2$. The considerable photocatalytic efficiency of the FeOOH/TiO$_2$ under visible light irradiation was therefore deduced to be caused by the hole transfer between the VB of FeOOH and TiO$_2$.

Key Words: Heterojunction, Photocatalyst, Visible light, FeOOH/TiO$_2$, FeOOH

Introduction

Remediation of environmental pollutants in water and air through photocatalytic reaction has drawn extensive interest over the last few decades.[1-3] Among various semiconductors, TiO$_2$ has been known as an excellent photocatalyst with its unique characteristics in band position and surface structure, as well as its extended chemical stability and non-toxicity.[4-7] TiO$_2$ can only utilize the photons in the UV region ($\lambda < 380$ nm) due to its large band gap ($E_g = 3.2$ eV), which limits its practical applications in sun light or indoor.[8-11]

In order to overcome this drawback, a new promising strategy would be the coupling of TiO$_2$ with other narrow bandgap semiconductors capable of harvesting the photons in the visible range.[12-14] Thus far numerous studies have been reported on the sensitizer-loaded TiO$_2$ showing photocatalytic activity under visible light irradiation, such as CdS/TiO$_2$, Cu$_2$O/TiO$_2$, CdSe/TiO$_2$, and others.[15-29] In most of these composites, the conduction band (CB) of the loaded sensitizer is located higher than that of TiO$_2$. Thus the electrons photogenerated by the sensitizer are transferred to CB of TiO$_2$ and these transferred electrons on TiO$_2$ can initiate various reduction reactions. We classified this as "type-A heterojunction" structure,[37] and this system will be eligible for the reduction reaction. In the oxidation reaction, however, the electrons in CB of TiO$_2$ can only lead to a partial decomposition of organic compound, and are difficult to induce CO$_2$ evolution.

Previously, we reported the FeTiO$_3$/TiO$_2$ system,[37] which is conceptually different from the conventional coupled photocatalysts. In this system, VB of FeTiO$_3$ and TiO$_2$ was very close. With a visible light irradiation FeTiO$_3$ is excited and its VB becomes partially vacant. Then, the hole in VB of FeTiO$_3$ can be transferred to that of TiO$_2$, and the holes induced in TiO$_2$ VB can be used to the oxidation of organic compounds as a result. We classified this system as "type-B heterojunction" and found that FeTiO$_3$/TiO$_2$ provides a high photocatalytic activity under visible light irradiation in evolving CO$_2$, which is evident for the complete mineralization.

FeOOH is considered to be an appropriate candidate for the construction of type-B heterojunction structure, since its VB is located lower than that of TiO$_2$ and its band gap of 2.6 eV allows sufficient visible light utilization.[30-33] In this work, we prepared the FeOOH/TiO$_2$ heterojunctions by coupling FeOOH and Degussa P25 nanoparticles using an organic linker. The photocatalytic behavior of FeOOH/TiO$_2$ composites in decomposing gaseous 2-propanol was investigated, and the mechanistic role of FeOOH was also discussed.

Experimental Section

Preparation of FeOOH/TiO$_2$ composites. Iron oxyhydroxide (FeOOH) was prepared by a hydrothermal reaction.[34-36] 100 mL of 3.0×10^{-2} M ferrous sulfate ($FeSO_4 \cdot 7H_2O$) aqueous solution was placed in a round-bottomed flask, and the separately prepared 100 mL aqueous solution containing 0.30 mmol hydroxylamine and 5.0 mmol ammonium acetate was added to this solution. The mixture was refluxed at 85 °C for 2 hr, and the created precipitate was washed with de-ionized water several times and dried overnight in air at 60 °C. The particle size of the synthesized FeOOH was ~100 nm.

For the formation of FeOOH/TiO$_2$ heterojunction structure, Degussa P25 with an average particle size of ~25 nm was chosen as the standard TiO$_2$. Typically, in preparing 2/98 FeOOH/TiO$_2$ (the composite consisting of 2 mol% FeOOH and 98 mol% TiO$_2$), 22.6 mg FeOOH and 1.00 g TiO$_2$ were separately suspended in each beaker containing 30 mL ethanol. 0.10 M maleic acid in 10 mL ethanol was added to the FeOOH suspension, and stirred vigorously for 5 hr. Then, the prepared TiO$_2$ suspension was poured to this solution, and vigorously stirred for another 10 hr. The suspension was precipitated by centrifugation, and the collected precipitate was dried overnight in air at 60 °C and subsequently annealed at 220 °C for 4 hr.

Characterization. X-ray diffraction (XRD) patterns were obtained for the FeOOH/TiO$_2$ powder samples by using a Rigaku Multiflex diffractometer with monochromated Cu K_α radiation. XRD scanning was performed under ambient conditions over the 2θ region of 15 - 60° at a rate of 2 °/min (40 kV, 20 mA). UV-visible diffuse reflectance spectra were acquired by a Perkin-Elmer Lambda 40 spectrophotometer. $BaSO_4$ was used as the reflectance standard. Transmission electron mi-

croscope (TEM) images were obtained by a Philips CM30 operated at 250 kV. One milligram of $FeTiO_3/TiO_2$ was dispersed in 50 mL of methanol, and a drop of the suspension was then spread on a holey amorphous carbon film deposited on the copper grid.

Evaluation of photocatalytic activity. The prepared FeOOH/TiO_2 samples were tested as visible light photocatalyst in decomposing 2-propanol in gas phase. 1.0 mL aqueous colloidal suspension containing 8.0 mg of FeOOH/TiO_2 (or other photocatalyst) was spread on a 2.5 × 2.5 cm^2 Pyrex glass in a smooth film form and subsequently dried at room temperature. The gas reactor system used for this photocatalytic activity has been described elsewhere.[38] For the measurement of photocatalytic activity under visible light, the whole FeOOH/TiO_2 film area was irradiated by a 300 W Xe lamp through a UV cut-off filter (< 420 nm, Oriel) and a water filter. After evacuating the reactor, 1.6 μL of 10% aqueous 2-propanol (v/v) was added to the 200 mL gas-tight reactor and the total pressure of the reactor was then controlled to 750 Torr by addition of oxygen gas. The gas mixtures in the reactor were magnetically convected during the irradiation. After a certain time of irradiation, 0.5 mL of the gas sample was automatically picked up from the reactor, and sent to a gas chromatograph (Agilent Technologies, Model 6890N). The remnant 2-propanol and evolved CO_2 during the photocatalytic reaction were monitored by a gas chromatography. For the detection of CO_2, a methanizer was installed between the GC column outlet and the FID detector.

Results and Discussion

Iron oxyhydroxide (FeOOH) particles were prepared by the reaction of Fe^{2+} salt with hydroxylamine in aqueous solution in the presence of ammonium acetate buffers. The average size of the synthesized FeOOH nanoparticle was ~100 nm, and most of particles were mutually separated without aggregation. For the formation of heterojunction structure, FeOOH and Degussa P25 nanoparticles were combined by introducing maleic acid as an organic linker, and the prepared sample was finally heat-treated at 220 °C to evaporate the organic components. Finally, UV light was irradiated for 4 hr to remove the residual organics in this system. TEM images, shown in Figure 1, describe the heterojunction structure of 2/98 FeOOH/TiO_2. It is shown that the TiO_2 nanoparticles in the size of ~25 nm were coupled to the large FeOOH particles, while some of them were mutually aggregated. The high resolution TEM images in Figure 1c and 1d suggest that a tight contact is formed between the TiO_2 and the large FeOOH particles.

Figure 2 shows the XRD patterns for the pure FeOOH, TiO_2 and FeOOH/TiO_2 heterojuction structures in different compositions. All the samples were heat-treated at 220 °C for 4 hr. In the pure FeOOH, the diffraction peaks appeared at 14.14°, 27.08°, 30.06°, 36.34°, 38.10°, and 46.86° correspond to the (020), (120), (011), (031), (111), and (200) peaks, respectively, of the orthorhombic FeOOH structure (JCPDS, No. 08-0098). In the Degussa P25 TiO_2, the diffraction peaks at 25.31°, 37.90°, 48.05°, and 53.95° correspond to the (101), (004), (200), and (105) peaks of the anatase phase, respectively, whereas the peaks at 27.49° and 36.15° correspond to the (110) and (101)

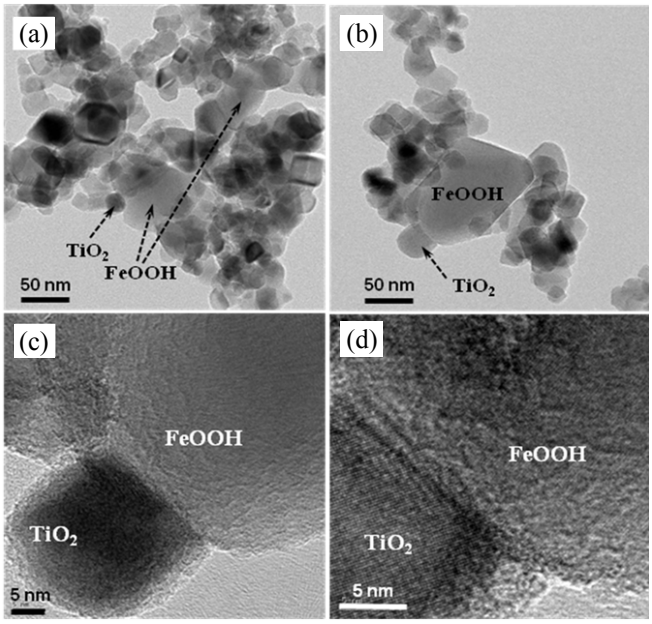

Figure 1. TEM images of the 2/98 FeOOH/TiO_2 heterojunction structures (a, b), and their high magnification TEM images (c, d).

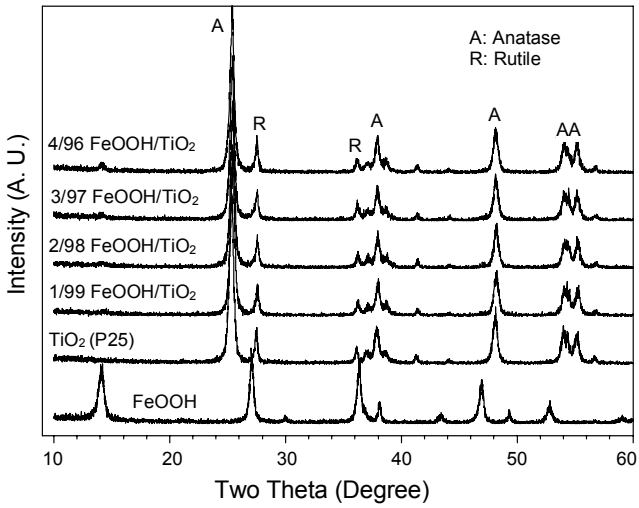

Figure 2. XRD patterns for FeOOH and TiO_2 (Degussa P25) nanoparticles, and FeOOH/TiO_2 heterojunction structures in several compositions.

peaks of the rutile phase, respectively. This suggests that the Degussa P25 is a mixed phase of the anatase and rutile. The diffraction peaks in Figure 2 also indicate that the FeOOH/TiO_2 composites are mixture of the orthorhombic FeOOH and TiO_2 with no impurity phases within detection limit, suggesting that there is no noticeable chemical reaction occurred between FeOOH and TiO_2 during the heat-treatment at 220 °C.

Figure 3 shows UV-visible diffuse reflectance spectra for TiO_2, FeOOH and several FeOOH/TiO_2. Owing to its wide band gap, TiO_2 shows a high reflectance in visible region, whereas FeOOH reveals a notably strong absorption up to the spectral range of ~550 nm. Therefore, the FeOOH/TiO_2 composites possess two different band edges at ~360 and ~550

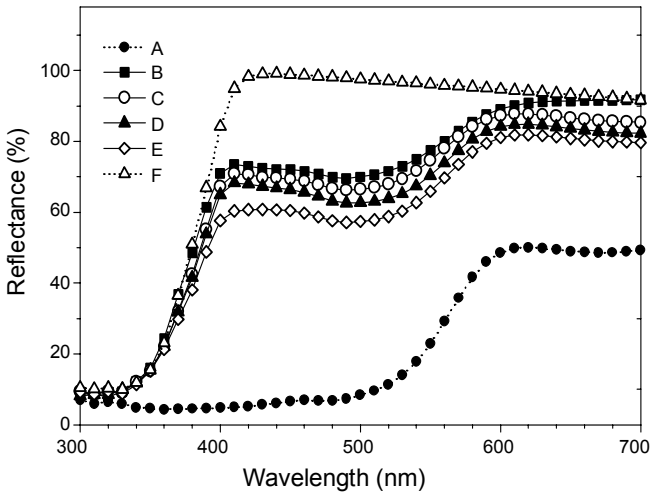

Figure 3. UV-visible diffuse reflectance spectra for FeOOH and TiO_2 (Degussa P25) nanoparticles, and FeOOH/TiO_2 heterojunction structures in several compositions. A, FeOOH; B, 1/99 FeOOH/TiO_2; C, 2/98 FeOOH/TiO_2; D, 3/97 FeOOH/TiO_2; E, 4/96 FeOOH/TiO_2; F, TiO_2.

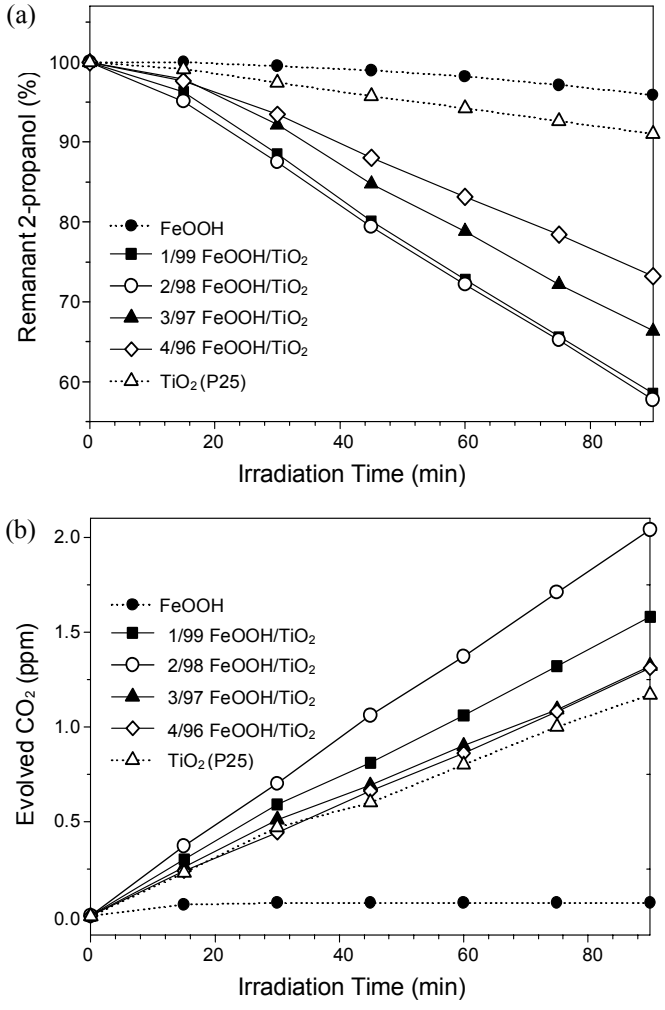

Figure 4. Photocatalytic decomposition of gaseous 2-propanol as a function of irradiation time. Percentage of remnant 2-propanol (a), and amount of CO_2 evolved (b).

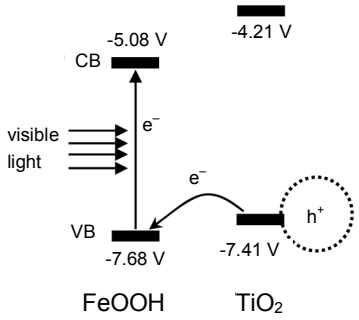

Figure 5. Schematic diagram describing the visible light photocatalytic reaction for the FeOOH/TiO_2 system. All potential levels were indicated versus vacuum level.

nm, and show significant absorption in the visible region up to ~550 nm. The absorbance was further enhanced with increasing FeOOH content. Notable absorption of the FeOOH/TiO_2 composites in the visible region implies efficient utilization of visible light for the photocatalytic reaction.

The photocatalytic activity of the FeOOH/TiO_2 composites in decomposing 2-propanol in gas phase was evaluated under a visible light irradiation ($\lambda \geq 420$ nm). As shown in Figure 4a, the photocatalytic activities of Degussa P25 and FeOOH were very low under visible light irradiation. By contrast, the FeOOH/TiO_2 composites in several compositions showed appreciably higher photocatalytic activity than their end-members. Especially, the 2/98 FeOOH/TiO_2 exhibits the highest photocatalytic activity. That is, about 42% of 2-propanol was decomposed after an irradiation of 90 min, whereas only 9.0% was decomposed by pure TiO_2 (Degussa P25). At higher concentration of FeOOH exceeding 2 mol%, the photocatalytic activity of the composites was gradually decreased.

The photocatalytic activity was also evaluated according to the amount of CO_2 evolved during the visible light irradiation. As shown in Figure 4b, several FeOOH/TiO_2 heterojunction structures reveal higher photocatalytic activity than the Degussa P25. The highest photocatalytic activity was observed from 2/98 FeOOH/TiO_2. After an irradiation of 90 min, the evolved CO_2 was 2.04 ppmv, which is approximately twice that of Degussa P25.

To enhance the photocatalytic activity of TiO_2, the coupling with other semiconductors has been frequently investigated in order to promote the separation of photogenerated charge carriers and/or to extend the absorption wavelength up to the visible region. In the present study, both TiO_2 and FeOOH showed a very low photocatalytic activity under a visible light irradiation, but their heterojunction showed notably enhanced photocatalytic activity. It is deduced that the high catalytic efficiency of the FeOOH/TiO_2 composite originates from the unique relative band positions of these two semiconductors.[30-33] Figure 5 describes a schematic diagram for the energy band position of FeOOH and TiO_2. Differently from most of semiconductors, VB level of FeOOH (–7.68 eV) is relatively lower than that of TiO_2 (–7.41 eV). Hence, the FeOOH/TiO_2 system is considered to be a typical example of type-B heterojunction structure. With visible light irradiation, the electrons in VB of FeOOH are excited to its CB, which induces partial vacancy in VB. Then, the

holes in VB of FeOOH can move to that of TiO_2, since VB of FeOOH is positioned lower than that of TiO_2. As a result, the holes generated in VB of TiO_2 can initiate various oxidation reactions. By this inter-semiconductor hole-transfer mechanism, the photogenerated charge carriers can be separated efficiently so that the composite can utilize the visible light to mineralize organic pollutants completely.

Conclusions

A visible light photocatalyst was formed by heterojunction between FeOOH and TiO_2. The 2/98 FeOOH/TiO_2 composite showed the highest photocatalytic activity in the decomposition of 2-propanol and evolution of CO_2 under visible light irradiation. Due to the unique band positions of these two semiconductors and the profound absorption of visible light by FeOOH, the FeOOH/TiO_2 composite exhibited high photocatalytic efficiency. Relatively lower VB level of FeOOH (–7.68 eV from vacuum level) than that of TiO_2 (–7.41 eV) enables the hole transfer from VB of FeOOH to that of TiO_2. As a result, the absorption of visible light by FeOOH induces the generation of holes in VB of TiO_2, which leads to the mineralization of organic compounds.

Acknowledgments. The authors gratefully acknowledge the financial support of Inha university.

References

1. Inoue, T.; Fujishima, A.; Konishi, S.; Honda, K. *Nature* **1979**, *277*, 637.
2. Hoffmann, M. R.; Martin, S. T.; Choi, W.; Bahnemann, D. W. *Chem. Rev.* **1995**, *95*, 69.
3. Chen, M.-L.; Bae, J.-S.; Oh, W.-C. *Bull. Korean Chem. Soc.* **2006**, *27*, 1423.
4. Ou, Y.; Lin, J.; Fang, S.; Liao, D. *Catal. Commun.* **2007**, *8*, 936.
5. Lee, S. H.; Kim, I. Y.; Kim, T. W.; Hwang, S.-J. *Bull. Korean Chem. Soc.* **2008**, *29*, 817.
6. Huang, Y.; Zheng, Z.; Ai, Z.; Zhang, L.; Fan, X.; Zou, Z. *J. Phys. Chem. B* **2006**, *110*, 19323.
7. Ding, Z.; Lu, G. Q.; Greenfield, P. F. *J. Phys. Chem. B* **2000**, *104*, 4815.
8. Song, K. Y.; Park, M. K.; Kwon, Y. T.; Lee, H. W.; Chung, W. J.; Lee, W. I. *Chem. Mater.* **2001**, *13*, 2349.
9. Zhao, W.; Ma, W.; Chen, C.; Zhao, J.; Shuai, Z. *J. Am. Chem. Soc.* **2004**, *126*, 13574.
10. Asahi, R.; Morikawa, T.; Ohwaki, T.; Aoki, K.; Taga, Y. *Science* **2001**, *293*, 269.
11. Sakthivel, S.; Kisch, H. *ChemPhysChem* **2003**, *4*, 487.
12. Kumar, A.; Mathur, N. *Appl. Catal. A* **2004**, *275*, 189.
13. Chai, S. Y.; Kim, Y. J.; Lee, W. I. *J. Electroceram.* **2006**, *17*, 909.
14. Ho, W.; Yu, J. C.; Lin, J.; Yu, J.; Li, P. *Langmuir* **2004**, *20*, 5865.
15. Ho, W.; Yu, J. C. *J. Mol. Catal. A: Chem.* **2006**, *247*, 268.
16. Bessekhouad, Y.; Chaoui, N.; Trzpit, M.; Ghazzal, N.; Robert, D.; Weber, J. V. *J. Photochem. Photobiol. A* **2006**, *183*, 218.
17. Song, H.; Jiang, H.; Liu, X.; Meng, G. *J. Photochem. Photobiol. A* **2006**, *181*, 421.
18. Pal, B.; Sharon, M.; Nogami, G. *Mater. Chem. Phys.* **1999**, *59*, 254.
19. Yin, H.; Wada, Y.; Kitamura, T.; Sakata, T.; Mori, H.; Yanagida, S. *Chem. Lett.* **2001**, *30*, 334.
20. Kumar, A.; Jain, A. *J. Mol. Catal. A: Chem.* **2001**, *165*, 265.
21. Chakraborty, A. K.; Chae, S. Y.; Lee, W. I. *Bull. Korean Chem. Soc.* **2008**, *29*, 494.
22. Liu, J.; Yang, R.; Li, S. *Rare Metals* **2006**, *25*, 636.
23. Jang, J. S.; Ji, S. M.; Bae, S. W.; Son, H. C.; Lee, J. S. *J. Photochem. Photobiol. A* **2007**, *188*, 112.
24. Yu, X.; Wu, Q.; Jiang, S.; Guo, Y. *Mater. Charact.* **2006**, *57*, 333.
25. Tristão, J. C.; Magalhães, F.; Corio, P.; Sansiviero, M. C. *J. Photochem. Photobiol. A* **2006**, *181*, 152.
26. Ge, L.; Xu, M.; Fang, H. *J. Mol. Catal. A: Chem.* **2006**, *258*, 68.
27. Kang, M. G.; Han, H. E.; Kim, K. J. *J. Photochem. Photobiol. A* **1999**, *125*, 119.
28. Jang, J. S.; Li, W.; Oh, S. H.; Lee, J. S. *Chem. Phys. Lett.* **2006**, *425*, 278.
29. Serpone, N.; Maruhamuthu, P.; Pichat, P.; Pelizzetti, E.; Hidaka, H. *J. Photochem. Photobiol. A* **1995**, *85*, 247.
30. Xu, Y.; Schoonen, M. *Am. Mineral.* **2000**, *85*, 543.
31. Schoonen, A. A.; Cohn, C. A.; Roemer, E.; Laffers, R.; Simon, S. R.; O'Riordan, T. *Rev. Mineral. Geochem.* **2006**, *64*, 179.
32. Grätzel, M. *Nature* **2001**, *414*, 338.
33. Linsebigler, A. L.; Lu, G.; Yates, J. T. *Chem. Rev.* **1995**, *95*, 735.
34. Ardizzone, S.; Formaro, L. *Surface Technol.* **1985**, *26*, 269.
35. Ardizzone, S.; Formaro, L.; Sivieri, E.; Burriesci, N.; Petrera, M. *J. Chem. Soc. Faraday Trans.1* **1983**, *79*, 2449.
36. Liu, X,; Qiu, G.; Yan, A.; Wang, Z.; Li, X. *J. Alloys Compd.* **2007**, *433*, 216.
37. Gao, B.; Kim, Y. J.; Chakraborty, A. K.; Lee, W. I. *Appl. Catal. B: Environ.* **2008**, *83*, 202.
38. Kwon, Y. T.; Song, K. Y.; Lee, W. I.; Choi, G. J.; Do, Y. R. *J. Catal.* **2000**, *191*, 192.